

# Beyond the coherent coupled channels description of nuclear fusion

M. Dasgupta<sup>1</sup>, D.J. Hinde<sup>1</sup>, A. Diaz-Torres<sup>1</sup>, B. Bouriquet<sup>1\*</sup>, Catherine I. Low<sup>1†</sup>, G.J. Milburn<sup>2</sup>, and J.O. Newton<sup>1</sup>

<sup>1</sup>*Department of Nuclear Physics, Research School of Physical Sciences and Engineering,  
Australian National University, Canberra, ACT 0200, Australia*

<sup>2</sup>*Department of Physics, University of Queensland, St. Lucia, QLD 4072, Australia*

(Dated: June 8, 2007)

New measurements of fusion cross-sections at deep sub-barrier energies for the reactions  $^{16}\text{O} + ^{204,208}\text{Pb}$  show a steep but almost saturated logarithmic slope, unlike  $^{64}\text{Ni}$ -induced reactions. Coupled-channels calculations cannot simultaneously reproduce these new data and above-barrier cross-sections with the same Woods-Saxon nuclear potential. It is argued that this highlights an inadequacy of the coherent coupled-channels approach. It is proposed that a new approach explicitly including gradual decoherence is needed to allow a consistent description of nuclear fusion.

PACS numbers: 25.70.Jj, 24.10.Eq, 03.65.Yz

Nuclear fusion involves a massive dynamical rearrangement of a complex quantum system having many degrees of freedom. To simplify the problem, the nuclear interactions are represented by a short-range attractive nuclear potential, which in combination with the long-range repulsive Coulomb potential, forms a barrier against fusion. In the simplest barrier-passing model of fusion, if the barrier is overcome, fusion occurs. This model failed to describe sub-barrier fusion of heavy nuclei [1, 2], demonstrating the need to include the effects of internal nuclear degrees of freedom explicitly [3]. The coupled channels model, including couplings between the relative motion of the colliding nuclei and their low energy collective excitations, successfully explained precisely measured fusion cross-sections at near-barrier energies [4].

A key ingredient in these calculations is the nuclear potential  $V_n$ , a construct to account for the many-body interactions between the protons and neutrons in the two nuclei that are not explicitly included through channel couplings. Commonly a Woods-Saxon form is used for the nuclear potential:  $V_n(r) = V_0[1 + \exp\{(r - R)/a\}]^{-1}$ , where  $V_0$ ,  $R$  and  $a$  are the depth, radius and the diffuseness parameters respectively. Since the Coulomb interaction is known exactly, the parameters of the nuclear potential determine the fusion barrier energy, the internuclear separation ( $r$ ) at which the barrier occurs (the barrier radius), and the width of the barrier. In practice, the parameters may be constrained by requiring that the calculations are consistent with fusion measurements [5]. They may also be taken from systematic parameterizations [6] of fits to scattering data. The latter give diffuseness parameters between 0.6 and 0.8 fm, in agreement with calculated values from the semi-microscopic double-folding potential [7]. However, above the barrier, calculations using these parameters systematically predict much higher fusion cross sections than those measured [8].

Only by using diffuseness parameters up to twice those expected can the experimental fusion data be reproduced [8]. Recent measurements of fusion cross-sections at energies far below the fusion barrier [9] have brought to light another problem – measured cross-sections fall much more rapidly than coupled channels predictions using standard nuclear potentials. A very shallow nuclear potential has been proposed [10, 11] to explain these measurements. However, as discussed later, at energies well-above the barrier this approach presents a significant logical problem, as the potential pocket disappears at higher angular momenta.

We present new experimental measurements of fusion cross-sections at deep sub-barrier energies for the reactions  $^{16}\text{O} + ^{204,208}\text{Pb}$ , complementing existing above-barrier measurements [12, 13]. Together they show that the coherent coupled channels approach is inadequate to describe fusion. It is argued that this approach is unrealistic as it implicitly assumes that energy dissipation (irreversibility) sets in at some point inside the barrier without affecting quantum coherence. It is proposed that a model with a gradual onset of decoherence between the superposed states is necessary to provide a robust solution to the problems of modelling nuclear fusion.

Pulsed beams ( $\simeq 1$  ns wide) of  $^{16}\text{O}$  in the energy range 74.0 – 102.0 MeV, provided by the ANU 14UD electrostatic accelerator, bombarded  $>99\%$  enriched targets of  $^{208}\text{PbS}$  and  $^{204}\text{PbS}$ , of  $\sim 90 \mu\text{g}/\text{cm}^2$  thickness, evaporated onto  $20 \mu\text{g}/\text{cm}^2$  C backings. The stability of the monitor energy spectra and count rates showed that target degradation was successfully minimized by limiting the beam current and translating the targets during the measurements. The compound nuclei formed following fusion decay mainly by fission, but a small part of the fusion yield results in evaporation residues.

Fission fragments were measured in coincidence using two large position sensitive multi-wire proportional counters [14]. Particle energy-loss, position and flight time with respect to the beam were recorded. The large difference in energy loss between beam-like particles and the fission fragments, together with kinematical coincidence requirements, resulted in essentially no background

---

\*Current address: C.E.R.F.A.C.S., 31057 Cedex 01, France

†Current address: Rangi Ruru Girls' School, Christchurch, New Zealand

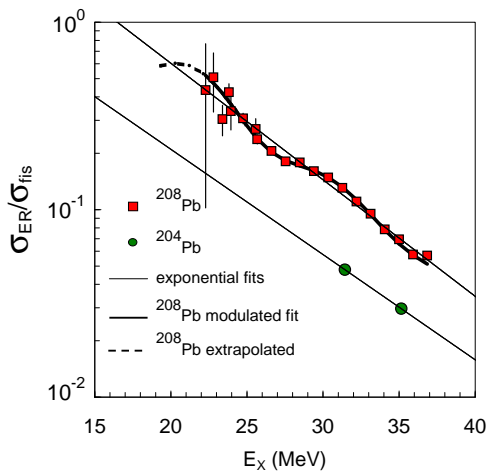


FIG. 1: (Color online) Ratio of evaporation residue to fission cross-sections as a function of excitation energy of the compound nucleus. The lines are fits to the data (see text).

events even at the lowest energy. Recoiling evaporation residues (ERs) were separated by a compact velocity filter [15], and then implanted into a silicon surface barrier detector, where they were uniquely identified by their  $\alpha$ -decay energies. Normalization of both the fission and ER measurements used Rutherford scattering, measured in two Si surface barrier monitor detectors placed symmetrically around the beam axis at forward angles.

After the fission measurements, the targets were analyzed for impurities at the ppb level using laser-ablation inductively-coupled plasma mass spectrometry [16]. The impurities in  $^{208}\text{Pb}$  that could lead to fission were below ppm levels, whilst 54 ppm of tungsten was found for  $^{204}\text{Pb}$ . Corrections were made by measuring fission from targets of the contaminant elements. Their contribution was only significant at the lowest energy for  $^{204}\text{Pb}$ , which required a correction of 14%, consistent with the experimental mean c.m. velocity of the fission events.

The fission cross-sections ( $\sigma_{fis}$ ) were measured down to centre of mass energies ( $E$ ) of 66 MeV and 67 MeV respectively for  $^{208}\text{Pb}$  and  $^{204}\text{Pb}$ , where  $\sigma_{fis} \sim 10^{-5}$  mb. Because of the lower efficiency, the ER cross-sections ( $\sigma_{ER}$ ) for  $^{208}\text{Pb}$  were only measured down to 69 MeV, where  $\sigma_{ER}$  is a few  $10^{-3}$  mb. At lower energies, they were estimated by extrapolating the measured  $\sigma_{ER}/\sigma_{fis}$ , which varies slowly with energy as shown in Fig.1. The thin full lines are the best-fitting exponentials, whilst the thick line is a modulation to the exponential fit to the  $^{208}\text{Pb}$  data that reproduces the discrete nature of the competition between fission and neutron evaporation. This function was used to extrapolate to the lowest energies for this reaction (short-dashed line). For the  $^{204}\text{Pb}$  reaction,  $\sigma_{ER}/\sigma_{fis}$  is smaller, and in both reactions variation of the extrapolations by 50% does not change the conclusions, as fission is the dominant decay mode. The fusion cross-sections ( $\sigma = \sigma_{fis} + \sigma_{ER}$ ) are shown in Fig.2, together with the results of previous

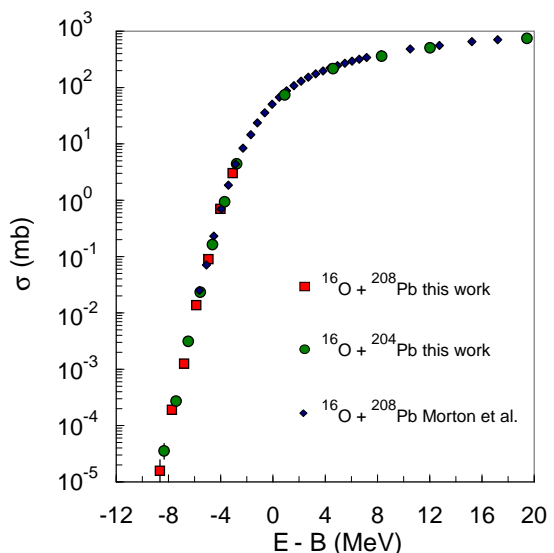


FIG. 2: (Color online) Fusion cross-sections as a function of the centre-of-mass energy with respect to the barrier energies  $B = 74.5$  and  $74.9$  MeV for  $^{208}\text{Pb}$  and  $^{204}\text{Pb}$  respectively.

measurements [12, 13] at higher energies. The two reactions are in excellent agreement, despite having different fission probabilities and target impurity corrections.

The two energy regions of interest here are well-below and well-above the barrier. Since comparing cross-sections on a logarithmic scale as in Fig.2 is not optimal, the results at the lowest energies are shown by taking the logarithmic slope  $d[\ln(E\sigma)]/dE$  [9] (allowing comparison of the tunnelling gradient independent of the weight of the lowest barrier), whilst cross-sections at above-barrier energies are shown on a linear scale. Neither the logarithmic slope at below-barrier energies, nor the energy dependence of the cross-sections well above the barrier depend on couplings. Nevertheless, comparisons are initially made with coupled channels calculations to demonstrate that the observed deviations are not due to inclusion or neglect of couplings.

The coupled channels calculations used the code CCFULL [17], with an ingoing wave boundary condition applied at the bottom of the ( $\ell$ -dependent) potential pocket inside the barrier. The Woods-Saxon nuclear potential depth and radius were chosen to match the calculated average barrier energy with that determined from experiment. Initial calculations used a diffuseness  $a = 0.66$  fm, consistent with double folding model calculations and the Woods-Saxon parametrization of the Aküz-Winther potential [6]. Couplings to the collective  $3^-$ ,  $5^-$  and double octupole phonon states (in the harmonic limit) in  $^{208}\text{Pb}$  were included [12].

The calculations are shown in Fig.3 by the dashed line. They do not match the initial rise of the experimental slope, indicating that the energy of the lowest barrier is not exactly reproduced. This is not unexpected in view of the inadequacies in our current understanding of the

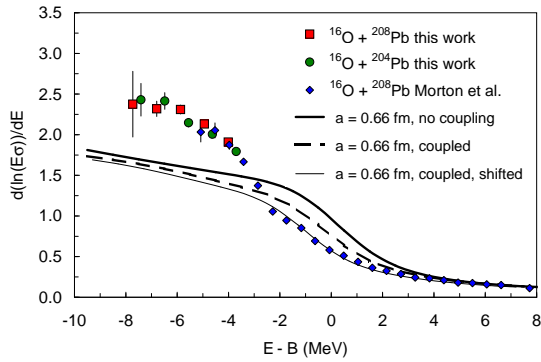


FIG. 3: (Color online) Logarithmic slope as a function of energy with respect to the barrier. Calculation with standard parameters fail to match the measurements at low energy.

couplings (particularly transfer) affecting fusion. Shifting the calculations down in energy by 0.8 MeV (thin full line) gives a good match to the rising part of the logarithmic slope. Importantly, this shift hardly changes the “saturation” logarithmic slope at the lowest energies, where both the measured and the calculated slopes vary slowly with energy. A calculation with no couplings (thick full line) shows the saturation slope is essentially unchanged by the couplings. Thus at deep sub-barrier energies, measurements can be compared with coupled channels calculations, shifted calculations or no-coupling calculations without affecting the conclusions. At these energies, the measured saturation slope lies well above those calculated, a consequence of the measured cross-sections falling more steeply with decreasing energy than the calculations. Similar disagreement has also been observed [9] for reactions of the heavier projectile  $^{64}\text{Ni}$ . There, however, no sign of saturation was found.

These calculations for  $^{16}\text{O} + ^{208}\text{Pb}$  also fail to reproduce the measured cross-sections at energies well-above the barrier, predicting much higher cross-sections, as shown in Fig.4(a). Calculations with (thin line) and without couplings (short dashed line) are almost identical, showing that this discrepancy is independent of whether couplings are included or not, as long as the calculated average barrier matches that measured. The above-barrier data can be reproduced using a larger value of the diffuseness parameter, as found in earlier works; a diffuseness  $a = 1.18$  fm (with  $V_0 = 300$  MeV) gives good agreement (dashed line in Fig.4(a)). These calculations, however, do not match the measured logarithmic slope at deep sub-barrier energies (dashed line in Fig.4(b)), which needs a diffuseness parameter of 1.65 fm, as shown by the thick line. Fig.4(a) shows that this completely fails to reproduce the above barrier cross-sections.

The failure to obtain a simultaneous description of the energy dependence of the below- and above-barrier fusion data, which are essentially unaffected by couplings, might be due to physical effects not being included. How could this affect both deep sub-barrier and above barrier fusion? At deep sub-barrier energies, the energy depen-

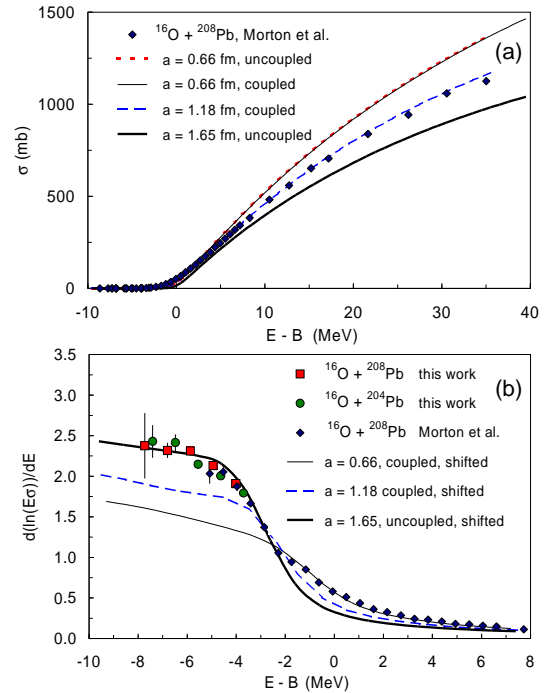


FIG. 4: (Color online) Calculations which reproduce  $\sigma$  above the barrier (a) fail to reproduce the low energy data (b).

dence of fusion cross-sections is determined by the width of the barrier. This is characterized by the outer and inner turning points. The above-barrier cross section at a particular energy is limited by the highest angular momentum ( $\ell\hbar$ ) that leads to fusion. In the model, this is determined by the corresponding high- $\ell$  barrier energy and radius, which is shifted to a smaller radius than the  $\ell = 0$  barrier by the repulsive centrifugal potential. Thus for a given energy below the barrier, the inner turning point is at the same separation distance as the top of the fusion barrier for a higher angular momentum [18]. This is true independent of the particular form of the nuclear potential (which is expected to be energy-independent over the 20–50 MeV energy range relevant here).

It follows that any *physical* mechanism invoked to reproduce the below-barrier measurements should also reproduce those above-barrier (and vice-versa). This has not been true of explanations put forth thus far. A shallow nuclear potential, which at smaller separations deviates from the Woods-Saxon form, has been used to explain deep sub-barrier fusion data [11]. This may be part of the explanation, but cannot be the complete picture, as a shallow potential leads to no trapping potential pocket for higher angular momenta. It is only by the application of an ingoing wave boundary condition at a fixed distance inside the barrier [11] that fusion occurs. However, this implies energy damping processes at that radius which should also affect tunnelling probabilities below the barrier. The use of large diffuseness values as empirical fit parameters for above-barrier data [5, 12] are not satisfactory either, as they fail to describe deep sub-barrier

fusion cross sections.

In the coherent coupled channels model, the total wave-function is written as a linear superposition of a (limited) number of basis states, which is subject to Hamiltonian unitary evolution. Capture, which in reality occurs through an irreversible loss of translational kinetic energy to the multitude of single particle degrees of freedom, is simulated by applying an ingoing wave boundary condition or a short-ranged imaginary potential. Although the model implicitly (and correctly) includes irreversibility some distance inside the barrier, the significant implication of irreversibility on the coherent superposition is neglected. Irreversibility cannot occur without decoherence, which rapidly transforms the linear superposition of state vectors into a mixed state described by a density matrix ( $\rho$ ):

$$|\psi\rangle = \alpha|\psi_1\rangle + \beta|\psi_2\rangle \Rightarrow \rho = |\alpha|^2|\psi_1\rangle\langle\psi_1| + |\beta|^2|\psi_2\rangle\langle\psi_2|.$$

Decoherence is fundamental to open quantum systems, and results from the interaction between the explicitly included degrees of freedom and other (typically many) degrees of freedom, called the environment [19, 20]. Increasing the size of the basis in the coherent coupled-channels approach (to include states identified with the environment) will not result in decoherence. Decoherence can be modelled in an explicitly time-dependent density matrix approach. The effects of decoherence in condensed matter physics and quantum optics are now well recognized [19–21]. Decoherence is often, but not always, associated with energy dissipation. It was demonstrated that dissipation decreases quantum tunnelling in the pioneering work of Ref. 22, where the environment was modeled as a large number of harmonic oscillators. In other systems, the environment is identified as the quasi continuum of states coupled to the quasi bound states of an unstable system, describing for example the decay of an optical cavity mode in quantum optics [23].

In nuclear fusion, the environment cannot be external to the two colliding nuclei. However, it is clear that the environmental degrees of freedom must fall outside the coupled channels model space, which describes an entirely coherent quantum system. Identifying the

environment with internal nucleonic degrees of freedom implies that couplings to the environment should have a strong radial dependence; this coupling could be direct, or through doorway states such as the giant resonances [24]. This immediately suggests that the environment acts as an effective position measurement of the radial coordinate. It gives a mechanism by which the resulting decoherence can change tunnelling rates, as demonstrated experimentally in atom optics [25], where the decay of a quasi-bound cold atom can be changed due to repeated observations of its position.

A gradual onset of decoherence [21] with increasing nuclear overlap may be thought of as making the system gradually more classical. In fusion, as beam energies are reduced further below the barrier, decoherence should increasingly suppress the sub-barrier fusion enhancement that results from the coherent superposition. It can also result in energy dissipation, giving angular momentum and energy loss for higher partial waves, which will change the above-barrier fusion cross sections.

This suggested approach differs from dynamical models up to now, which have been formulated in the extreme limits of a completely coherent quantum picture where no energy dissipation can occur, or have included dissipation classically, semiclassically or using statistical concepts. To our knowledge there is no quantum dynamical model of nuclear reactions that explicitly includes decoherence, although the first steps in this direction have been taken using the Lindblad equation [26]. Such a model would naturally include system-environment couplings, and provide an avenue to reconcile the coherent coupled-channels model with classical models of energy dissipation which describe deep-inelastic scattering. It may even have significant implications for astrophysical (low energy) fusion reactions, where the inner turning point is far inside the barrier.

We thank K. Hagino and J.A. Tostevin for illuminating discussions, C.M. Allan for assisting with target composition measurements, C.R. Morton and A.C. Berriman for assistance during initial ER measurements and R.A. Yanez in the fission measurements. M.D. and D.J.H. acknowledge the support of an ARC Discovery Grant.

- 
- [1] R.G. Stokstad *et al.*, Phys. Rev. C **21**, 2427 (1980).  
 [2] A.B. Balantekin *et al.*, Phys. Rev. C **28**, 1565 (1983).  
 [3] C.H. Dasso *et al.*, Nucl. Phys. **A405**, 381 (1983); **A407**, 221 (1983).  
 [4] M. Dasgupta *et al.*, Annu. Rev. Nuc. Part. Sci. **48**, 401 (1998).  
 [5] J.R. Leigh *et al.*, Phys. Rev. C **52**, 3151 (1995).  
 [6] R.A. Broglia and A. Winther, Heavy Ion Reactions, Vol.I, Benjamin/Cummings, Reading, Massachusetts, 1981.  
 [7] I.I. Gontchar *et al.*, Phys. Rev. C **69**, 024610 (2004).  
 [8] J.O. Newton *et al.*, Phys. Lett. B **586**, 219 (2004); Phys. Rev. C **70**, 024605 (2004).  
 [9] C.L. Jiang *et al.*, Phys. Rev. Lett. **93**, 012701 (2004).  
 [10] C.H. Dasso and G. Pollarolo, Phys. Rev. C **68**, 054604 (2003).  
 [11] Ş. Mişicu and H. Esbensen, Phys. Rev. Lett. **96**, 112701 (2006).  
 [12] C.R. Morton *et al.*, Phys. Rev. C **60**, 044608 (1999).  
 [13] D.J. Hinde *et al.*, Phys. Rev. Lett. **89**, 0282701 (2002).  
 [14] D.J. Hinde *et al.*, Phys. Rev. C **53**, 1290 (1996).  
 [15] J.X. Wei *et al.*, Nucl. Instrum. Methods Phys. Res. **A306**, 557 (1991).  
 [16] G.F. Durrant, J. Anal. At. Spectrom. **14**, 1385 (1999).  
 [17] K. Hagino, N. Rowley, and A.T. Kruppa, Comput. Phys. Commun. **123**, 143 (1999).  
 [18] M. Dasgupta *et al.*, FUSION06, AIP Conference Proceed-

- ings **853**, 21 (2006).
- [19] C. Kiefer and Erich Joos, *Quantum Future: Proceedings of the Xth Max Born Symposium*, Springer-Verlag, Berlin, p.105 (1999), arXiv:quant-ph/9803052v1.
- [20] M. Schlosshauer, *Decoherence and the quantum-to-classical transition*, Springer Verlag, (2007).
- [21] P. Sonnentag and F. Hasselbach, Phys. Rev. Lett. **98**, 200402 (2007).
- [22] A.O. Caldeira and A.J. Leggett, Phys. Rev. Lett. **46**, 211 (1981).
- [23] G.J. Milburn and D.F. Walls, *Quantum Optics*, Chapter 16, Springer, Berlin (1994).
- [24] R.A. Broglia *et al.*, Phys. Lett. **B61**, 113 (1976).
- [25] M.C. Fischer, B. Gutierrez-Medina and M.G. Raizen, Phys. Rev. Lett. **87**, 040402 (2001).
- [26] M. Genkin and W. Scheid, J. Phys. G **34**, 441 (2007).